# Photoswitching of monomeric and dimeric DNA-intercalating cyanine dyes for super-resolution microscopy applications†

**Cristina Flors***

*Received 1st October 2009, Accepted 14th January 2010*
*First published as an Advance Article on the web 10th February 2010*
**DOI: 10.1039/b9pp00119k**

A growing trend in far-field super resolution fluorescence microscopy based on single molecule photoswitching involves the replacement of photoactivatable fluorophores by common organic dyes in which photoswitching reactions or blinking can be induced. This alternative strategy can greatly simplify the sample preparation and imaging scheme in some cases, and enables its application to a wider range of biological systems. This methodology has been applied successfully to unveil the nanoscale organisation of proteins, but little progress has been seen to date in DNA super-resolution imaging. Previous results have shown that blinking can be induced in the DNA-intercalating dimeric dye YOYO-1 in combination with a reducing buffer, and in turn super-resolution images of DNA can be reconstructed. However, monomeric intercalating dyes like YO-PRO-1 are more advantageous for biological applications. This paper shows that both YO-PRO-1 and YOYO-1 can be used in super-resolution imaging, and different sample preparation strategies are compared in terms of spatial resolution and homogeneity of the reconstructed super-resolution images. Moreover, ensemble and single-molecule experiments provide insight into the switching mechanism. The dyes YOYO-1 and YO-PRO-1 hold great potential for their use in nanoscale imaging of DNA topology in biology and nanoscience.

## Introduction

Fluorescence microscopy is a widespread and indispensable tool in biological and materials sciences. However, light diffraction limits its spatial resolution to about 200 nm in the imaging plane, precluding the study of sub-cellular structures. A group of techniques have recently emerged that are able to overcome this limit and achieve spatial super-resolution, enabling the study of cellular organisation at the nanoscale.[1–4] Some of these super-resolution techniques, such as (fluorescence) photoactivation-localisation microscopy (PALM,[5] fPALM[6]) and stochastic optical reconstruction microscopy (STORM)[7] rely on the possibility of switching fluorescent labels between on- and off-states. PALM, STORM and related techniques[8–11] are based on cycles of stochastic switching, detection and localisation of single-molecules on a wide-field microscope. Fluorescence photoswitching is thus in the core of these powerful imaging techniques, and there is increased interest in finding new photoswitches for super-resolution imaging, based on both organic dyes and fluorescent proteins. A recent trend aims at the simplification of the imaging scheme, namely by circumventing the use of photoswitchable fluorophores as such and inducing switching reactions in conventional (*i.e.* non-photoswitchable or non-photoactivatable) organic fluorophores[8,12–19] or fluorescent proteins.[16,17,20] Nanoscale imaging with standard fluorophores can be thus performed by taking advantage of the formation of long-lived dark states (photoblinking), which may be formed by photoinduced electron transfer between organic dyes and redox-active buffers,[14,18,19] reversible addition of thiyl radicals,[21,22] or by light-induced flickering of fluorescent proteins.[23,24] This strategy involves switching the majority of the fluorophores to a metastable state and recording those that remain or have spontaneously returned to the fluorescent state. Organic fluorophores such as rhodamine 6G, Atto, Cy and Alexa dyes have successfully been used to generate super-resolution images with this approach.

The above strategies have mainly been applied to image the nanoscale organisation of proteins by targeting dye-labelled antibodies or by fusions with fluorescent proteins. However, there is still a need to find a methodology to image DNA topology at the nanoscale and so far there has been little progress in this direction.[7,17,25] A high density of (photo)switchable fluorophores is needed, since this parameter is directly related to the resolution that can be achieved. Previous results have shown that the use of DNA intercalating cyanine dyes in a reducing buffer is a promising option for super-resolution imaging based on single-molecule photoswitching.[26] These dyes are very bright when intercalated into DNA, but their fluorescence is essentially zero when free in solution.[27] This greatly reduces the fluorescence background generated by unbound molecules and is particularly advantageous for this imaging technique. It was shown that the formation of metastable dark states could be induced in the green dye YOYO-1, presumably by photoinduced electron transfer reactions between a reducing buffer containing β-mercaptoethylamine (MEA) or by the guanosine bases in DNA. A spatial resolution below 40 nm for stretched λ-DNA was achieved with a low cost setup consisting of a front-illuminated EMCCD camera.[26] This methodology holds

*School of Chemistry and Collaborative Optical Spectroscopy Micromanipulation & Imaging Centre (COSMIC), University of Edinburgh, Joseph Black Building, The King's Buildings, West Mains Rd., EH9 3JJ, Edinburgh, United Kingdom. E-mail: cristina.flors@ed.ac.uk; Fax: +44 (0)131 650 6453; Tel: +44 (0)131 650 4713*

† Electronic supplementary information (ESI) available: Fig. S1: Selected CCD frames from single molecule experiments in the same conditions as those in Fig. 2. See DOI: 10.1039/b9pp00119k

great potential for its application to any field where DNA topology and organisation is important. For some biological applications, however, a drawback of YOYO-1 and other dimeric intercalating dyes is that binding of DNA is extremely strong ($K = 10^8$–$10^9$ $M^{-1}$),[28] which influences its topology and in turn its ability to interact with DNA-binding proteins. Indeed, dimeric intercalating dyes have been shown to inhibit significantly the activity of enzymes such as exo- and endo-nucleases[29,30] and DNA helicases,[31] with a degree of inhibition dependent on the dye/bp (dye to base pair) ratio. Monomeric intercalating dyes, which induce a smaller unwinding of DNA upon binding,[32] are an alternative in this case, and DNA-binding enzymes are indeed significantly less inhibited by these fluorophores.[31] YO-PRO-1, in contrast to YOYO-1 or other dyes, has also been shown to be a useful probe for bacteriophage T5, as it penetrates the phage capsid without damaging it and efficiently binds the DNA inside.[33] Moreover, although both YOYO-1 and YO-PRO-1 are considered to be impermeant to cells,[28,34] the latter dye can pass through the membrane of apoptotic cells[35] and through certain receptor channels in live cells,[36] which would be an advantage for imaging of cellular DNA.

The brightness of monomeric dyes is about half that of their dimeric counterparts, and their affinity to DNA is about two orders of magnitude lower.[28] This paper explores the photoswitching and photoblinking properties of monomeric and dimeric DNA-intercalating cyanine dyes in reducing buffers, and how these photophysical processes can be exploited in super-resolution imaging of DNA.

## Experimental

The oxazole yellow and thiazole orange dyes YOYO-1, TOTO-3 and YO-PRO-1 were purchased from Invitrogen. Immobilised λ-DNA (New England Biolabs) was prepared as described previously.[26] Briefly, 60–80 μL of a solution of DNA (1 μg in 250 μl) were deposited onto a polylysine-coated coverslip, and allowed to bind for about 20 s. The sample was then spin-coated at 5000 rpm. While the sample was spinning, 4 ml of water were pipetted onto the centre of the coverglass, to allow the water flow to stretch the DNA, and to remove unbound material.[37]

The coverglasses with DNA were then attached to a CoverWell imaging chamber (Grace Bio Labs), which contained "switching buffer": 10 mM phosphate buffered saline (PBS, pH 7.4, Sigma P3813) with an oxygen scavenger (0.5 mg $ml^{-1}$ glucose oxidase (Sigma), 40 μg $ml^{-1}$ catalase (Sigma) and 10% w/v glucose (Fischer Scientific)) and 50 mM β-mercaptoethylamine (MEA, Fluka).[8] In some cases, λ-DNA was labelled prior to the spincoating step at the appropriate dye/bp ratio, as in previous experiments ("method 1").[26] Alternatively, labelling was carried out after spincoating, by adding the dye into the imaging buffer (30 nM for YO-PRO-1 and 3 nM for YOYO-1) ("method 2"). For the latter experiments, the dye/bp ratio could thus not be reliably estimated. The single molecule samples of YOYO-1 and TOTO-3 shown in Fig. 2 were prepared using method 1 at a dye/bp ratio of 1 : 1600 and 1 : 20, respectively. For YO-PRO-1 (Fig. 2c), the sample was prepared by method 2 with a dye concentration of 150 pM in switching buffer.

Fluorescence imaging was performed on a Nikon Eclipse TE2000 inverted microscope, equipped with a total internal reflection fluorescence (TIRF) oil-immersion objective (Apochromat, 60×, NA 1.49, Nikon). Excitation was provided by a 488 nm CW Ar+ laser (163-C, Spectra-Physics, 0.5 kW $cm^{-2}$) or a 633 nm He/Ne CW laser (Coherent model #31-2140-000, 1 kW $cm^{-2}$ at the sample) passing through appropriate bandpass filters (Chroma Technology). Wide-field illumination was achieved by focusing the expanded and collimated laser beam onto the back-focal plane of the objective. The resulting illuminated area was roughly about 60 μm in diameter. Emission was collected by the same objective and imaged by an Andor iXon DV887 EMCCD camera after passing through a dichroic mirror (z488rdc or z633rdc, Chroma Technology) and additional spectral filters (HQ500LP and HQ530/50, or HQ645LP and HQ700/75, Chroma Technology). Additional lenses resulted in a final pixel size of 78–98 nm. Integration time per frame was 100 ms, and the total number of frames collected was typically 3000. The images were analysed with an Igor Pro routine by fitting Gaussian functions to individual molecules and localising their centre. Images in Fig. 3 were reconstructed by dividing each pixel into subpixels and assigning each localisation to a subpixel. The image brightness thus represents the density of localisations in a subpixel.

The number of photons detected was estimated from the fluorescence counts in a background-corrected image of a single molecule. Fluorescence counts were converted to into photons by using the electron per A/D count conversion and electron multiplying (EM) gain factors provided by the manufacturer. The values shown are rough estimates as the camera used has non-linear EM gain.

## Results and discussion

### Bulk measurements of fluorescence (photo)activation

The switching ability of the intercalating dyes bound to DNA was first quantified in a bulk experiment, and the effect of different buffer conditions on the fluorescence recovery was tested. Fig. 1 shows the photobleaching behaviour of YOYO-1 and YO-PRO-1 intercalated into DNA with an excitation power of about 0.5 kW $cm^{-2}$, and the fluorescence recovery after 160 s in the dark. Photobleaching was partially reversible in all cases, and the extent of the reversibility depended on the buffer. First, a comparison can be made between samples prepared by method 1 (see Experimental section) (Fig. 1, top panel). In the presence of MEA and in the absence of oxygen (switching buffer) fluorescence recovery of YOYO-1 was on average more efficient (38%) than when both MEA and oxygen were present (23%), or in PBS (15%). Recovery of the fluorescence could not be accelerated by irradiation at 633 nm, a wavelength that was not absorbed by the ground state of YOYO-1. The red intercalating dye TOTO-3 was also investigated in switching buffer, and a 30% recovery was found (not shown).

Another comparison can be made with the samples prepared by method 2 (Fig. 1, bottom panel). This method was used as YO-PRO-1 was washed away in the spincoating step due to its lower binding affinity to DNA. Switching buffer was used in these experiments since it provided the highest degree of fluorescence recovery, as seen in the above experiment. In this case, the recovery varied throughout different regions of the sample, with a maximum apparent recovery of 74% for YOYO-1 and 61% for YO-PRO-1. About 38% of this recovery is possibly due to reversible switching, as found in YOYO-1 samples prepared by method

 

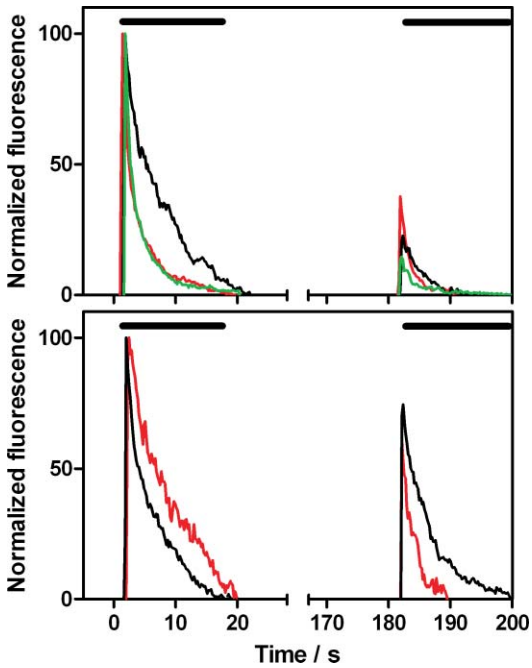


**Fig. 1** Bulk photobleaching (488 nm, 0.5 kW cm$^{-2}$) and fluorescence recovery after 160 s in the dark. Top: YOYO-1 in PBS (green), switching buffer (red) and 50 mM MEA (black) prepared by method 1 (1 : 20 dye/bp). Bottom: YOYO-1 (black) and YO-PRO-1 (red) samples prepared by method 2 in switching buffer. Black horizontal bars represent periods when the 488 nm laser is exciting the sample.

1. Further staining of dye-free DNA regions probably accounts for the rest of the observed fluorescence recovery. It is worth mentioning that photobleached YOYO-1 does not significantly loose its affinity to bind DNA, so it does not detach to allow fresh YOYO-1 molecules to intercalate.[38]

As previously proposed, photoinduced electron transfer between YOYO-1 and MEA, guanosine or guanosine bases that have been previously oxidised (8-oxo-7,8-dihydro-2′-deoxyguanosine, 8-oxo-dGuo) might be partly responsible, in the first instance, for the reversible photoswitching reaction.[26,38] Interestingly, 15% recovery in the dark was still observed in PBS, suggesting a role of guanosine or 8-oxo-dGuo in the switching reaction, in addition to the effect of MEA. With a reduction potential of about –1.30 V *vs.* SCE, YOYO-1 can spontaneously undergo photoinduced electron transfer with guanosine and thiol compounds with $\Delta G^0 = -0.35$ and –0.56 eV, respectively, calculated from its excited singlet state and at pH 7.4.[39,40] Following the electron transfer reaction with any of the electron donors, subsequent charge migration through DNA and trapping in certain sites might be responsible for the stabilisation of the observed dark states.

On a secondary note, Fig. 1 (top panel) shows that the fluorescence photobleaching phase of YOYO-1 in switching buffer from 1–20 s is biexponential. Biexponential bleaching of YOYO-1 in solution has been shown at higher dye/bp ratios (>1 : 4) and reflects different binding modes of the dye to DNA.[38] However, in the present study, the dye/bp ratio of 1 : 20 is not high enough to expect two binding modes. This biexponential bleaching curve might reflect different photobleaching mechanisms of YOYO-1 in immobilised DNA depending on its immediate environment.

The comparison between the black and red curves in the top panel of Fig. 1 shows that, even though the presence of molecular oxygen decreases the fluorescence recovery, it also arrests photobleaching of YOYO-1. This observation suggests that the triplet state of this dye is involved in the photobleaching mechanism (either irreversible, reversible, or both). The involvement of the triplet state might be promoted by the presence of the heavy atom iodine as a counterion, which enhances intersystem crossing. The triplet lifetime of YOYO-1 intercalated into DNA has been estimated as 10 μs by fluorescence correlation spectroscopy,[41] but there is no information about its triplet energy and the spontaneity for photoinduced electron transfer reactions from this state cannot be quantified.

### Single-molecule characterisation of intercalating cyanine dyes

Single-molecule microscopy had previously shown photoblinking of YOYO-1 in switching buffer upon excitation by 488 nm light, with an heterogeneous duration of dark states.[26] Herein, this behaviour is confirmed (Fig. 2a, and S1A in the ESI†), and it is possible to roughly estimate the number of photons detected in the on-state as 600–3200 by using a more sensitive CCD camera than in previous experiments.[26] In the case of the red dimeric dye TOTO-3, it is expected that its detection at the single-molecule

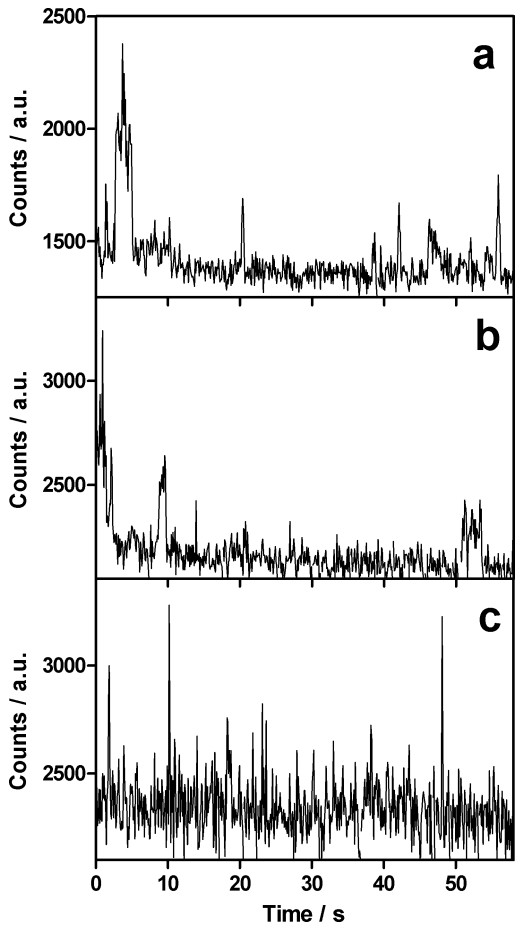


**Fig. 2** Single-molecule fluorescence trajectories (100 ms bin time) of YOYO-1 (a), TOTO-3 (b) and YO-PRO-1 (c) in switching buffer showing the formation of long-lived dark states. In (a) and (c) excitation was at 488 nm, and in (b) at 633 nm.[43]

level will be difficult due to its low brightness ($\varepsilon = 154\,000\ M^{-1}\ cm^{-1}$, $\Phi_F = 0.06$),[28] but blinking of this dye could still be detected upon irradiation with 633 nm light (Fig. 2b and S1B†). Fluorescence bursts consisted typically of about 400 photons, but more than 2000 photons could be detected in some cases. The latter number is higher than expected considering the 5-fold lower brightness of TOTO-3 compared to YOYO-1 ($\varepsilon = 98\,900\ M^{-1}\ cm^{-1}$, $\Phi_F = 0.52$).[28] However, the degree of labelling appeared to be lower for TOTO-3 than for YOYO-1, even though the same dye/bp ratio was used and both dyes have similar affinity to DNA.[28] This suggests that most of the TOTO-3 molecules could not be detected by the camera, and only the very bright molecules such as the one in Fig. 2b could be recorded. This would point to some effect of the DNA sequence on the photophysical properties of TOTO-3, which has been shown for other dyes in the same family.[39] TOTO-3 is thus not suitable for super-resolution imaging due to its low brightness. It was also found that TOTO-3 induced precipitation of DNA at 1 : 20 dye/bp when attempting to stretch the labelled DNA on the coverslip. Similar dyes such as TOTO-1[42] and BOBO-3 (C. Flors, unpublished) have been shown to induce DNA precipitation due to cross-linking or cross-intercalation.

For both YOYO-1 and TOTO-3, the fluorescence traces in Fig. 2 are consistent with their dimeric nature, showing brighter events at the beginning of the traces followed by bursts about half of the intensity, presumably after photobleaching of one chromophoric unit. As discussed above, the nature of the observed long dark states might be a charge-separated state that originates from the triplet state of the dyes and that is stabilised by migration along the DNA and trapping.

Fig. 2c shows a typical trace for YO-PRO-1, which is rather different to those of the above dimeric dyes (see also Fig. S1C†). Fluorescence bursts were much shorter, with a typical duration of hundreds of milliseconds, and contained less photons (300–900), consistent with a 2-fold lower brightness and a two orders of magnitude lower binding affinity to DNA compared to YOYO-1 ($K \approx 10^6\ M^{-1}$).[44] The photophysical properties of YO-PRO-1 are quite similar to those of YOYO-1, which suggests that the sharp fluorescent spikes in Fig. 2c might be the result of a highly dynamic association and dissociation of YO-PRO-1 to DNA resulting from the lower binding constant. The similarity between the traces of YOYO-1 and TOTO-3, both with bursts lasting for a few seconds, is consistent with this hypothesis. Indeed, both dimeric dyes have different fluorescence properties but similar affinity to DNA. In addition to binding and unbinding events, photoinduced electron transfer reactions might also contribute to the observed blinking in YO-PRO-1, similarly to the case of YOYO-1.

### Super-resolution imaging based on single-molecule photoswitching

As shown in the previous section, the studied dyes are able to form long-lived dark states on the order of seconds, which is an appropriate timescale for single-molecule switching super-resolution microscopy. It was previously reported that it is possible to reconstruct super-resolution images of YOYO-1 in DNA with a spatial resolution below 40 nm.[26] Fig. 3a shows the super-resolution reconstructed image of stretched λ-DNA labelled with YOYO-1 prepared by method 1. The use of a more sensitive camera improves the resolution slightly to 34 nm, as estimated from the full-width-at-half-maximum (FWHM) of a Gaussian fit to a cross-section line (Fig. 3c, blue curve). The image appears, however, quite heterogeneous, mainly due to the detachment of some dye in the spincoating step.

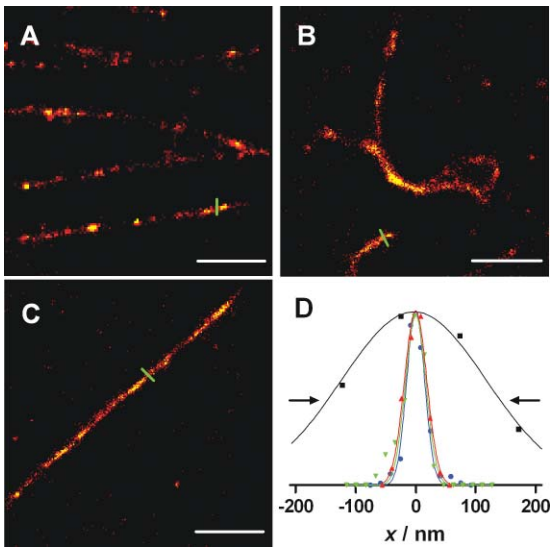


**Fig. 3** Super-resolution reconstructed images of stretched λ-DNA labelled with YOYO-1 (A) and (B) and YO-PRO-1 (C). Sample in panel (A) was prepared using method 1 and samples in panels (B) and (C) using method 2. Scale bar 1 μm. (D) Wide-field diffraction-limited cross-section (black) compared with super-resolution image cross-sections corresponding to panel A (blue), B (green) and C (red). The Y-axis represents the normalised density of localisations of line cross-sections (green bars in A–C), except for the black curve, which represents standard fluorescence intensity of a cross-section. Arrows indicate FWHM.

On the other hand, the YOYO-1/DNA images obtained with sample preparation method 2 (3 nM dye in switching buffer) resulted in a much better homogeneity, and more features are visible (Fig. 3b). The spatial resolution achieved in this case is just below 40 nm, probably due to the higher fluorescence background produced by the free dye in the imaging buffer.

It is also possible to reconstruct super-resolution images of DNA labelled with YO-PRO-1 (sample preparation method 2, 30 nM dye in switching buffer), as shown in Fig. 3c. Compared to YOYO-1, the degree of staining appears to be much lower, and thus a 10× concentration of free dye in the solution is needed. The average cross-section in this case is estimated as 43 nm. The lower resolution is expected due to the lower brightness, DNA affinity and higher background in the solution. The image of the DNA strand in Fig. 3c also shows good homogeneity.

Attempts were made to use PBS instead of switching buffer in the imaging chamber. However, irreversible photobleaching of YOYO-1 and YO-PRO-1 was too high and not enough blinking events could be recorded to reconstruct satisfactory images, as suggested by the low fluorescence recovery of 15% shown in Fig. 1.

It is worth noting that non-specific adsorption of all dyes to the glass surface could be observed, as the dyes become transiently bright upon immobilisation. This does not affect significantly the final reconstructed images, as the density of events is much higher in the regions where DNA is present.

 

## Conclusions

DNA-intercalating cyanine dyes have several advantages for their use in super-resolution imaging of DNA topology, mainly their commercial availability in a broad spectral range and simple labelling procedure. This paper shows that both green monomeric YO-PRO-1 and dimeric YOYO-1 can be used for single-molecule switching microscopy in combination with reducing buffers. In the case of YO-PRO-1, the blinking events might be a combination of photoinduced switching reactions, most probably by electron transfer, and dynamic binding and unbinding to DNA. Moreover, it is shown that for both YO-PRO-1 and YOYO-1 the homogeneity of the super-resolution images can be improved by adding free dye in the imaging buffer, at the cost of increasing the fluorescence background and thus the localisation accuracy of the single molecules. The red dye TOTO-3, on the other hand, is not a suitable candidate for multicolour super-resolution imaging due to its low brightness and the induction of DNA aggregation.

The green intercalating dyes studied show great potential for unveiling the nanoscale organisation of DNA in either DNA-based nanotechnology and some biological applications. YO-PRO-1 has advantages in terms of biological compatibility with DNA-binding proteins and for cell imaging.

## Acknowledgements

This work has been supported by the EPSRC Life Sciences Interface program (EP/F042248/1) and the RASOR grant from the BBSRC (BB/C511599/1). Dr Peter Dedecker (Katholieke Universiteit Leuven, Belgium) is gratefully acknowledged for providing the data analysis software.

## Notes and references

1 S. W. Hell, Far-field optical nanoscopy, *Science*, 2007, **316**, 1153.
2 M. Heilemann, P. Dedecker, J. Hofkens and M. Sauer, Photoswitches: Key molecules for subdiffraction-resolution fluorescence imaging and molecular quantification, *Laser Photonics Rev.*, 2009, **3**, 180.
3 B. Huang, M. Bates and X. Zhuang, Super-resolution fluorescence microscopy, *Annu. Rev. Biochem.*, 2009, **78**, 993.
4 J. Lippincott-Schwartz and S. Manley, Putting super-resolution fluorescence microscopy to work, *Nat. Methods*, 2009, **6**, 21.
5 E. Betzig, G. H. Patterson, R. Sougrat, O. W. Lindwasser, S. Olenych, J. S. Bonifacino, M. W. Davidson, J. Lippincott-Schwartz and H. F. Hess, Imaging intracellular fluorescent proteins at nanometer resolution, *Science*, 2006, **313**, 1642.
6 S. T. Hess, T. P. K. Girirajan and M. D. Mason, Ultra-high resolution imaging by fluorescence photoactivation localization microscopy, *Biophys. J.*, 2006, **91**, 4258.
7 M. J. Rust, M. Bates and X. W. Zhuang, Sub-diffraction-limit imaging by stochastic optical reconstruction microscopy (STORM), *Nat. Methods*, 2006, **3**, 793.
8 M. Heilemann, S. van de Linde, M. Schüttpelz, R. Kasper, B. Seefeldt, A. Mukherjee, P. Tinnefeld and M. Sauer, Subdiffraction-resolution fluorescence imaging with conventional fluorescent probes, *Angew. Chem., Int. Ed.*, 2008, **47**, 6172.
9 C. Geisler, A. Schönle, C. von Middendorff, H. Bock, C. Eggeling, A. Egner and S. W. Hell, Resolution of l/10 in fluorescence microscopy using fast single molecule photo-switching, *Appl. Phys. A: Mater. Sci. Process.*, 2007, **88**, 223.
10 J. S. Biteen, M. A. Thompson, N. K. Tselentis, G. R. Bowman, L. Shapiro and W. E. Moerner, Super-resolution imaging in live Caulobacter crescentus cells using photoswitchable EYFP, *Nat. Methods*, 2008, **5**, 947.
11 C. Flors, J. I. Hotta, H. Uji-i, P. Dedecker, R. Ando, H. Mizuno, A. Miyawaki and J. Hofkens, A Stroboscopic Approach for Fast Photoactivation-Localization Microscopy with Dronpa Mutants, *J. Am. Chem. Soc.*, 2007, **129**, 13970.
12 S. van de Linde, U. Endesfelder, A. Mukherjee, M. Schüttpelz, G. Wiebusch, S. Wolter, M. Heilemann and M. Sauer, Multicolor photoswitching microscopy for subdiffraction-resolution fluorescence imaging, *Photochem. Photobiol. Sci.*, 2009, **8**, 465.
13 S. van de Linde, R. Kasper, M. Heilemann and M. Sauer, Photoswitching microscopy with standard fluorophores, *Appl. Phys. B: Lasers Opt.*, 2008, **93**, 725.
14 C. Steinhauer, C. Forthmann, J. Vogelsang and P. Tinnefeld, Superresolution Microscopy on the Basis of Engineered Dark States, *J. Am. Chem. Soc.*, 2008, **130**, 16840.
15 D. Baddeley, I. D. Jayasinghe, C. Cremer, M. B. Cannell and C. Soeller, Light-induced dark states of organic fluochromes enable 30 nm resolution imaging in standard media, *Biophys. J.*, 2009, **96**, L22.
16 J. Folling, M. Bossi, H. Bock, R. Medda, C. A. Wurm, B. Hein, S. Jakobs, C. Eggeling and S. W. Hell, Fluorescence nanoscopy by ground-state depletion and single-molecule return, *Nat. Methods*, 2008, **5**, 943.
17 P. Lemmer, M. Gunkel, Y. Weiland, P. Muller, D. Baddeley, R. Kaufmann, A. Urich, H. Eipel, R. Amberger, M. Hausmann and C. Cremer, Using conventional fluorescent markers for far-field fluorescence localization nanoscopy allows resolution in the 10-nm range, *J. Microsc.*, 2009, **235**, 163.
18 J. Vogelsang, T. Cordes, C. Forthmann, C. Steinhauer and P. Tinnefeld, Controlling the fluorescence of ordinary oxazine dyes for single-molecule switching and superresolution microscopy, *Proc. Natl. Acad. Sci. U. S. A.*, 2009, **106**, 8107.
19 M. Heilemann, S. van de Linde, A. Mukherjee and M. Sauer, Super-resolution imaging with small organic fluorophores, *Angew. Chem., Int. Ed.*, 2009, **48**, 6903.
20 M. Gunkel, F. Erdel, K. Rippe, P. Lemmer, R. Kaufmann, C. Hormann, R. Amberger and C. Cremer, Dual color localization microscopy of cellular nanostructures, *Biotechnol. J.*, 2009, **4**, 927.
21 S. van de Linde, M. Sauer and M. Heilemann, Subdiffraction-resolution fluorescence imaging of proteins in the mithocondrial inner membrane with photoswitchable fluorophores, *J. Struct. Biol.*, 2008, **164**, 250.
22 G. T. Dempsey, M. Bates, W. E. Kowtoniuk, D. R. Liu, R. Y. Tsien and X. Zhuang, Photoswitching Mechanism of Cyanine Dyes, *J. Am. Chem. Soc.*, 2009, **131**, 18192.
23 G. U. Nienhaus and J. Wiedenmann, Structure, Dynamics and Optical Properties of Fluorescent Proteins: Perspectives for Marker Development, *ChemPhysChem*, 2009, **10**, 1369.
24 H. E. Seward and C. R. Bagshaw, The photochemistry of fluorescent proteins: implications for their biological applications, *Chem. Soc. Rev.*, 2009, **38**, 2842.
25 C. Steinhauer, R. Jungmann, T. L. Sobey, F. C. Simmel and P. Tinnefeld, DNA origami as a nanoscopic ruler for super-resolution microscopy, *Angew. Chem., Int. Ed.*, 2009, **48**, 8870.
26 C. Flors, C. N. J. Ravarani and D. T. F. Dryden, Super-resolution imaging of DNA labelled with intercalating dyes, *ChemPhysChem*, 2009, **10**, 2201.
27 B. A. Armitage, Cyanine dye-DNA interactions: Intercalation, groove binding, and aggregation, *DNA Binders and Related Subjects*, 2005, **253**, 55.
28 R. P. Haugland, M. T. Z. Spence, I. D. Johnson and A. Basey, The Handbook–A Guide to Fluorescent Probes and Labeling Technologies, *Molecular Probes*, 2005, 269–273.
29 X. Meng, W. W. Cai and D. C. Schwartz, Inhibition of restriction endonuclease activity by DNA binding fluorochromes, *J. Biomol. Struct. Dyn.*, 1996, **13**, 945.
30 S. Matsuura, J. Komatsu, K. Hirano, H. Yasuda, K. Takashima, S. Katsura and A. Mizuno, Real-time observation of a single DNA digestion by lambda exonuclease under a fluorescence microscope field, *Nucleic Acids Res.*, 2001, **29**, 79e.
31 C. Xu, M. Y. Losytskyy, V. B. Kovalska, D. V. Kryvorotenko, S. M. Yarmoluk, S. McClelland and P. R. Bianco, Novel, monomeric cyanine dyes as reporters for DNA helicase activity, *J. Fluoresc.*, 2007, **17**, 671.
32 A. Furstenberg and E. Vauthey, Ultrafast excited-state dynamics of oxazole yellow DNA intercalators, *J. Phys. Chem. B*, 2007, **111**, 12610.
33 M. Eriksson, M. Hardelin, A. Larsson, J. Bergenholtz and B. Akerman, Binding of intercalating and groove-binding cyanine dyes to bacteriophage T5, *J. Phys. Chem. B*, 2007, **111**, 1139.

34 T. V. Votyakova, A. S. Kaprelyants and D. B. Kell, Influence of Viable Cells on the Resuscitation of Dormant Cells in Micrococcus luteus Cultures Held in an Extended Stationary Phase: the Population Effect, *Appl. Environ. Microbiol.*, 1994, **60**, 3284.
35 T. Idziorek, J. Estaquier, F. De Bels and J. C. Ameisen, YOPRO-1 permits cytofluorometric analysis of programmed cell death (apoptosis) without interfering with cell viability, *J. Immunol. Methods*, 1995, **185**, 249.
36 A. D. Michel, R. Kaur, I. P. Chessell and P. P. Humphrey, Antagonist effects on human P2X(7) receptor-mediated cellular accumulation of YO-PRO-1, *Br. J. Pharmacol.*, 2000, **130**, 513.
37 M. Tanigawa and T. Okada, Atomic force microscopy of supercoiled DNA structure on mica, *Anal. Chim. Acta*, 1998, **365**, 19.
38 C. Kanony, B. Akerman and E. Tuite, Photobleaching of asymmetric cyanines used for fluorescence imaging of single DNA molecules, *J. Am. Chem. Soc.*, 2001, **123**, 7985.
39 T. L. Netzel, K. Nafisi, M. Zhao, J. R. Lenhard and I. Johnson, Base-Content Dependence of Emission Enhancements, Quantum Yields, and Lifetimes for Cyanine Dyes Bound to Double-Strand DNA: Photophysical Properties of Monomeric and Bichromomphoric DNA Stains, *J. Phys. Chem.*, 1995, **99**, 17936.
40 E. Madej and P. Wardman, The oxidizing power of the glutathione thiyl radical as measured by its electrode potential at physiological pH, *Arch. Biochem. Biophys.*, 2007, **462**, 94.
41 M. Shimizu, S. Sasaki and M. Kinjo, Triplet fraction buildup effect of the DNA-YOYO complex studied with fluorescence correlation spectroscopy, *Anal. Biochem.*, 2007, **366**, 87.
42 J. P. Jacobsen, J. B. Pedersen, L. F. Hansen and D. E. Wemmer, Site selective bis-intercalation of a homodimeric thiazole orange dye in DNA oligonucleotides, *Nucleic Acids Res.*, 1995, **23**, 753.
43 The background levels are different between panel (a) and (c) due to slightly different EM gain settings and also due to the different sample preparation conditions. In the case of panel (b), it is not possible to draw a comparison with the others as the wavelength range is different.
44 J. T. Petty, J. A. Bordelon and M. E. Robertson, Thermodynamic characterization of the association of cyanine dyes with DNA, *J. Phys. Chem. B*, 2000, **104**, 7221.

 